NASA TN D-966

TECHNICAL NOTE

D-966

EFFECT OF DECARBURIZATION ON NOTCH SENSITIVITY AND FATIGUE-CRACK-PROPAGATION RATES IN 12 MoV STAINLESS-STEEL SHEET

By William H. Herrnstein III and Arthur J. McEvily, Jr.

Langley Research Center
Langley Air Force Base, Va.

NATIONAL AERONAUTICS AND SPACE ADMINISTRATION

WASHINGTON November 1961

NATIONAL AERONAUTICS AND SPACE ADMINISTRATION

TECHNICAL NOTE D-966

EFFECT OF DECARBURIZATION ON NOTCH SENSITIVITY AND FATIGUE-CRACK-PROPAGATION RATES IN 12 MoV STAINLESS-STEEL SHEET

By William H. Herrnstein III and Arthur J. McEvily, Jr.

SUMMARY

Tests were conducted in order to determine the effect of surface decarburization on the notch sensitivity and rate of fatigue crack propagation in 12 MoV stainless-steel sheet at room temperature. Three specimen configurations were utilized in the course of the investigation: standard tensile specimen, 9-inch-wide specimens containing fatigue cracks or thread-cut notches of 0.005-inch radius, and 2-inch-wide specimens containing fatigue cracks. The 12 MoV stainless-steel sheet in the normal condition was found to have an ultimate tensile strength of 251 ksi and to be extremely notch sensitive. The material in the decarburized condition was found to have an ultimate tensile strength of 210 ksi and to be considerably stronger than the normal material in the presence of fatigue cracks. Decarburization did not appear to have any significant influence on the rate of fatigue crack propagation in the 2-inch-wide specimens at the stress levels considered. In addition to the tests, two methods for predicting residual static strength and their application to the material are discussed.

INTRODUCTION

The notch sensitivity of high-strength steels is a matter of concern in the design of critical structures such as missile cases. Cracks may develop in these structures as a result of flaws, poor welding technique, or low cycle fatigue. It has been suggested (refs. 1 and 2) that this notch sensitivity may be lowered through surface decarburization. Decarburization, while reducing notch sensitivity, also reduces the high static strength; therefore, a balance between these two effects would have to be reached in order to obtain an optimum design. In addition, since the growth of fatigue cracks to critical size is of concern, the effect of decarburization on the rate of fatigue crack propagation must be considered.

The present paper presents the results of an investigation aimed at evaluating these factors for a material of known high notch sensitivity, 12 MoV stainless steel.

SYMBOLS

a	half-length of internal notch, in.
E_n	secant modulus for nominal stress on net section, ksi
E_u	secant modulus corresponding to point of maximum stress on stress-strain curve, ksi
G_c	material constant, critical crack extension force for onset of fast crack propagation, lb/in.
K_E	theoretical stress concentration factor for ellipse
K_H	theoretical stress concentration factor for circular hole
K_N	theoretical stress concentration factor modified for size effect
K_u	stress concentration factor for ultimate tensile strength, S_u/S_{nu}
R	ratio of minimum stress to maximum stress in fatigue cycle
S	nominal stress on net section, ksi
S_{net}	maximum load in fatigue cycle divided by remaining net sectional area, ksi
S_{nu}	maximum load in static fracture test divided by the net section area immediately prior to the static fracture test, ksi
S_o	maximum load in fatigue cycle divided by initial net sectional area, ksi
S_u	ultimate tensile strength of material, ksi
w	width of specimen, in.
ρ	radius of curvature at notch root, in.
ρ'	Neuber material constant, in.
ρ_e	effective radius of curvature at notch root, in.

MATERIAL, SPECIMENS, AND TESTS

Material

Type 12 MoV stainless-steel sheet was chosen for this investigation primarily for its pronounced static notch sensitivity to sharp cracks at room temperature. The material was supplied by the manufacturer in the form of two sheets having nominal thicknesses of 0.025 inch and 0.031 inch. The nominal composition is given in table I.

The material was heat treated according to the schedule given in table II. The 0.025-inch sheet was decarburized (fig. 1) to an extent which varied somewhat over the surface of the sheet by austenitizing in air. In order to avoid decarburization, the 0.031-inch sheet was austenitized in a hydrogen atmosphere (fig. 1). The material in the nondecarburized condition will hereafter be referred to as normal.

Specimens

Three specimen configurations were utilized in the course of this investigation. All specimens were cut with the load axis parallel to the rolling direction.

Standard sheet tensile specimens.- The standard sheet tensile specimen (fig. 2(a)), which complies with ASTM standards (ref. 3), was used for the determination of the mechanical properties and stress-strain curves of the material in both the decarburized and normal conditions. After machining and prior to testing, the faces and edges of these specimens were dry polished with 3/0 emery paper in order to remove the heat treating scale and to insure notch-free surfaces.

Static strength specimens.- Notched 9-inch-wide specimens (fig. 2(b)) were tested in order to evaluate the static notch sensitivity of the material in each condition. One-half of these specimens contained an internal notch of arbitrary length with a notch root radius of 0.005 inch; the rest contained a fatigue crack which was grown from an internal notch of arbitrary length.

Notches (fig. 2(b)) were prepared by first cutting to within approximately 0.030 inch of the desired length of cut with a jeweler's saw. The 0.005-inch radius was then formed by repeatedly drawing a nylon thread impregnated with a fine grinding compound across the notch root. The fatigue cracks were initiated and grown from the thread-cut notches under axial tension loads with $R \approx 0$. The nominal stresses at which the cracks were grown ranged between 22 and 138 ksi depending upon the length of the saw cut in the specimen.

Crack propagation specimens.- Notched 2-inch-wide specimens (fig. 2(b)) were tested to determine the rate of fatigue crack propagation as a function of stress for the material in both the decarburized and normal conditions. Prior to testing, the region of the specimen in the vicinity of the notch was polished in order to facilitate observation of the crack as it propagated. Scribe marks were placed perpendicular to the path of the crack at measured intervals in order that the growth could be measured during the test with the aid of a 30× microscope and stroboscopic illumination.

Tests

Three types of tests were involved in this investigation. All tests were conducted at room temperature.

Standard tensile.- A number of standard tensile tests were conducted such that a reliable average of the mechanical properties of the material in each condition might be established. The strain rate in these tests was approximately 0.2 percent per minute.

Residual static strength.- The residual static strength of the 9-inch-wide specimens containing internal notches was determined by tension loading the specimens to failure in a 120,000-pound-capacity hydraulic testing machine. Guide plates were used to prevent localized buckling at the stress raiser due to transverse compressive stresses in tests on the normal specimens. Very little buckling was observed, however, in the tests on decarburized specimens without guide plates. Aside from this difference, the tests on the decarburized and normal specimens in this investigation were conducted in the same manner. The strain rate for all tests was approximately 0.2 percent per minute.

Crack propagation.- The fatigue crack propagation tests were conducted under axial load with notched 2-inch-wide specimens in both the decarburized and normal conditions. The fatigue machines used are of the subresonant type with nominal capacity of ±20,000 pounds. The machines are equipped with auxiliary hydraulic loading systems for applying high loads at reduced speeds (ref. 4). As in the case of the residual static strength tests, the normal specimens were restrained from buckling by guide plates.

Fatigue cracks were initiated at the notch roots in all specimens by cycling hydraulically at S_o = 60 ksi with $R \approx 0$. The fatigue crack was then propagated to failure at constant load amplitude with $R \approx 0$ at S_o = 60, 50, 40, 30, or 20 ksi. Two specimens in each condition were tested at each stress level with two exceptions. The exceptions were the stress levels of 40 and 20 ksi at which only one

specimen of the normal material was tested. At the stress levels of 60, 50, and 40 ksi the cycling was performed hydraulically at speeds not exceeding 20 cpm. At the lower stress levels the cycling was performed mechanically at a speed of approximately 1,800 cpm.

In order to start crack growth at the stress levels of 30 and 20 ksi after initiation at the higher stress, it was necessary to cycle the specimens for a time at each of a series of progressively lower stresses approaching the stress at which the crack was propagated. This procedure was necessary because the residual compressive stresses developed at the tip of the fatigue crack at a high stress level will retard crack growth at some lower stress level if the difference in the two stress levels is large (ref. 5).

RESULTS

Standard Tensile

The results of the standard tensile tests are presented in table III for the material in both the decarburized and normal conditions. A typical stress-strain curve for the material in each condition is shown in figure 3. The properties of the decarburized material were subject to an amount of scatter significantly greater than that associated with the normal material. This is reflected in the larger scatter range for the ultimate strength as given in the table. It should be noted that the percent elongation for the material in the normal condition is significantly lower than has been reported elsewhere for this material of similar thickness. Elongations of 10.5 percent in 2 inches are reported for 0.050-inch-thick sheet in reference 6.

Failures were of the brittle type with the fracture surfaces perpendicular to the specimen edges for the most part. In two instances, specimens of the normal material shattered into three pieces at failure.

Residual Static Strength

The results of the residual static strength tests are presented in table IV and are shown in figure 4.

In figure 4 the residual static strength S_{nu} is plotted as a function of crack length for all the 9-inch-wide specimens tested. This figure indicates that short cracks result in large reductions in residual static strength for the material in either the decarburized or normal conditions. In addition, this figure shows that the percent reduction

in strength is, as would be expected, a function of the severity of the notch. The reduction is greater for the specimens containing fatigue cracks than for specimens containing thread-cut notches regardless of the crack length or condition of the material.

The specimens failed in a consistent manner with one exception. The cracks initiated at the notch roots and propagated immediately in a direction normal to the edge of the specimens until failure was complete. The exception was specimen 1 of the normal material which shattered into several pieces at failure. No slow crack growth was observed in any test.

Crack Propagation

The results of the crack propagation tests are shown in figure 5. The crack lengths given in the figure are the averages for the specimens tested at each propagation stress level. The curves were plotted from a common crack length at each stress level in order to facilitate comparison between the material in the decarburized and normal conditions. The stress levels were chosen to provide data over a wide range of fatigue life.

In general, the cracks grew in a symmetric fashion. No tearing or stepwise growth was observed until failure was imminent.

DISCUSSION

Standard Tensile Tests

The effect of decarburization on the mechanical properties of 12 MoV stainless steel is readily seen in table III. The material in the decarburized condition has a lower yield strength and ultimate tensile strength but is slightly more ductile. In this discussion it is assumed that the 6-mil difference in sheet thickness contributes negligibly to the observed differences in strength and ductility. This assumption would seem reasonable in view of the fact that no difference in ductility and only a difference of approximately 6 ksi in ultimate strength have been observed for 0.100-inch- and 0.050-inch-thick 12 MoV stainless-steel sheet (ref. 6). The observed differences, therefore, will be attributed to decarburization.

It has been mentioned previously that the extent of decarburization was not uniform from specimen to specimen. This nonuniformity in all liklihood accounts for the greater scatter evident in the results of tests on decarburized specimens.

Residual Static Strength Tests

The effect of decarburization on the notch sensitivity of 12 MoV stainless-steel sheet can be seen in figures 4, 6, and 7. In figures 6 and 7, the residual-static-strength data are presented with S_{nu} plotted as a percent of S_u, the ultimate strength. (The curves on the figure will be explained and discussed subsequently.) Comparison of the data points in figures 6 and 7 indicates that the notch sensitivity to 0.005-inch thread-cut notches is about the same in decarburized and normal material except for the point for the longest notch in the normal material. This point, corresponding to normal specimen 8, is very low and will be discussed later. However, the decarburized material is decidedly less notch sensitive to fatigue cracks. Indeed, S_{nu}/S_u for decarburized material is more than twice that of the normal material over most of the fatigue crack range. Figure 4 indicates that the absolute load-carrying capacity of the decarburized material containing fatigue cracks exceeds that of the normal material, particularly in the short-crack range. It appears, then, that even though the ultimate tensile strength is reduced, decarburization of such materials can be beneficial particularly in applications where short fatigue or welding cracks must be tolerated.

The applicability of methods of analysis developed for the prediction of residual static strength to the data obtained for 12 MoV stainless steel was an additional consideration in this investigation. The two methods considered were the methods proposed in references 7 and 8. The former may be called the stress-concentration method; the latter, the Griffith-Irwin method.

The stress-concentration method is based upon the calculation of the maximum local stress in the specimen. The elastic stress concentration factor for a symmetric elliptical hole in a sheet under tension is computed by using the following modification of the expression for the stress concentration at a hole in a sheet of finite width:

$$K_E = 1 + (K_H - 1)\sqrt{\frac{a}{\rho}} \tag{1}$$

The elastic factor is then modified for size by using the relation

$$K_N = 1 + \frac{K_E - 1}{1 + \sqrt{\frac{\rho'}{\rho}}} \tag{2}$$

In the case of a crack, which is considered as an elongated ellipse, an effective radius ρ_e is used for ρ (ref. 7). The factor K_N, when modified for plasticity effects, results in the following expression for the stress concentration factor at fracture:

$$K_u = \frac{S_u}{S_{nu}} = 1 + \left(K_N - 1\right)\frac{E_u}{E_n} \tag{3}$$

Application of equation (3) requires evaluation of the quantities ρ_e, ρ', and E_u/E_n. The quantity E_u/E_n was found from the stress-strain curve. Its value for stresses below the yield stress was found to be 0.161 for the normal material and 0.114 for the decarburized material. As in reference 7, ρ' was calculated from the results of tests of specimens containing notches of known radii (0.005 inch) by using equations (1), (2), and (3). This value of ρ' was then used to calculate ρ_e from tests of specimens containing fatigue cracks.

When this approach was attempted in analyzing the present data it was found that a value of $\rho' = 0.02$ inch was necessary to obtain agreement between the theory and the experimental data for the normal specimens containing 0.005-inch notches. The next step was to use this value of ρ' and compute ρ_e for the specimens containing fatigue cracks by means of equations (1), (2), and (3). However, when this approach was attempted it was found that even for $\rho_e \to 0$ the values of K_N were not large enough to bring the data and predictions into agreement. The reason for this is that the expression for K_N (eq. (2)), approaches a limiting value as ρ_e approaches zero, such that K_N is a function of ρ'. This relationship is given in the following equation:

$$K_N = 1 + \left(K_H - 1\right)\sqrt{\frac{a}{\rho'}} \tag{4}$$

Since it appeared that ρ_e was much less than ρ', equation (4) was applied to the fatigue-crack data, and a value of $\rho' = 0.0015$ inch was obtained for the normal material. Similarly, a value of $\rho' = 0.005$ inch was obtained for the decarburized material. These values were adopted in the present analysis and were used for both the thread-cut and fatigue crack predictions of static strength.

The stress-concentration-method predictions using these values of ρ' are shown as the solid lines in figures 6 and 7. In general, agreement between theory and data is only fair. It is seen in figure 6 that the theory is unable to account for the large difference in static strength between the thread-cut and fatigue crack specimens of the

L
1
3
5
4

normal material. It is also seen that good agreement with the theory was obtained for the normal specimens containing fatigue cracks. The agreement in figure 7 is satisfactory except for the exaggeration of the influence of short cracks by the theory. It is seen in figure 6 that one point, corresponding to normal specimen 8, is decidedly low in comparison with the rest of the data for thread-cut notches. As seen in figure 4, this is the only point which opposes the trend that normal specimens are stronger than decarburized specimens containing 0.005-inch notches. Consequently, it is felt that this particular data point should be viewed with suspicion.

The Griffith-Irwin method of analysis requires the determination of a material constant G_c, which is defined as the critical crack extension force for the onset of fast crack propagation. If S_{nu} is below the yield stress and if the crack length is not more than one-half the specimen width, G_c for a centrally notched sheet in tension is defined by the expression:

$$G_c = \frac{\left[S_{nu}(w - 2a)\right]^2}{Ew} \tan \frac{\pi a}{w} \qquad (5)$$

where E is the modulus of elasticity measured in ksi. This equation is further restricted to plane stress conditions and to cases where the notches have sharp roots and propagate rapidly to fracture. Therefore, in this investigation the equation is applicable to only the fatigue cracked specimens.

The constant G_c was calculated by using the experimental S_{nu} for specimens 9 and 12 for the decarburized and normal material, respectively. The value was found to be 157 lb/in. for the decarburized material and 64 lb/in. for the normal material.

With the values of G_c thus determined, the predicted residual static strength as a function of crack length was computed for the material in each condition by using equation (5). The predictions are shown as the dashed curves in figures 6 and 7. As can be seen, the two methods predict similar results for this material.

Crack Propagation Tests

The effects of decarburization on fatigue crack propagation in 12 MoV stainless-steel sheet are shown in figure 5. The decarburized specimens were able to sustain a longer crack prior to failure at all but one of the stress levels at which the cracks were propagated. This reflects the

fact that the material in this condition is less notch sensitive. In general, decarburization had no significant influence on crack propagation rate or fatigue life at a given level of S_o. The differences observed are considered to be of the order of the range of scatter in the data. Inspection of the specimens after failure revealed that the crack fronts were farther advanced at the center of the fracture cross section than they were at the surface. It may be, then, that the condition of the core of the sheet is more important than the condition of the surface in crack propagation. On the other hand, the condition of the surface should be a matter of concern in static failure since plastic deformation over a larger area and the entire sheet thickness is involved.

In figure 8 the crack propagation rate is plotted as a function of $K_N S_{net}$ for the decarburized and normal specimens at each stress level. The analysis and method used to arrive at the figure are fully described in reference 9. The stress concentration factor K_N was computed by using equation (4) with the value of ρ' (0.0015 inch) obtained in the residual static strength tests on normal specimens. The selection of this one value of ρ' for the material in both conditions is felt to be justified since, as has been previously mentioned, the surface condition of the sheet has no significant effect on crack-propagation rates in this material. The crack-propagation rates presented refer to the progress of only one end of the crack relative to the center line of the specimen.

The curves in figure 8 exhibit more scatter than did similar curves for aluminum alloys (ref. 9). However, reasonable predictions of fatigue-crack-propagation rate for a given net stress and crack length are possible for the material in either condition. Included in the data is a short curve plotted from fatigue-crack-growth data taken for normal specimen 12 prior to static testing. The good agreement with the 2-inch-wide specimens is evident, and it indicates that the method may be used to predict rates of fatigue crack propagation in specimens of widths other than those employed in the test series.

CONCLUDING REMARKS

Type 12 MoV stainless-steel sheet in the normal condition has been found to be extremely notch sensitive to fatigue cracks at room temperature. Notch strengths as low as one-tenth of the ultimate tensile strength were obtained. Surface decarburization reduces this high notch sensitivity, but, accompanying this decrease, there is also a decrease in ultimate tensile strength. The load-carrying capacity of decarburized material when fatigue cracks are present is greater than that of normal

material tested under the same conditions. In specific applications of this material, decarburization may be desirable in order to reduce the notch sensitivity even though some tensile strength is sacrificed.

Studies of fatigue crack propagation have shown that, at a given stress level, there is no significant difference between the rates of fatigue crack propagation in normal and decarburized specimens.

Langley Research Center,
National Aeronautics and Space Administration,
Langley Air Force Base, Va., August 10, 1961.

REFERENCES

1. Lynch, John M.: For Stronger Missile Cases...Decarburize! Metal Progress, vol. 79, no. 3, Mar. 1961, pp. 78-81.

2. Shank, M. E., Spaeth, C. E., Cooke, V. W., and Coyne, J. E.: Solid-Fuel Rocket Chambers for Operation at 240,000 Psi. and Above - I. Metal Progress, vol. 76, no. 5, Nov. 1959, pp. 74-81.

3. Anon.: Tentative Methods of Tension Testing of Metallic Materials. ASTM Designation: E 8-57T. Pt. 3 of 1953 Book of ASTM Standards. ASTM (Philadelphia), 1958, pp. 103-119.

4. Naumann, Eugene C., Hardrath, Herbert F., and Guthrie, David E.: Axial-Load Fatigue Tests of 2024-T3 and 7075-T6 Aluminum-Alloy Sheet Specimens Under Constant- and Variable-Amplitude Loads. NASA TN D-212, 1959.

5. Schijve, J.: Fatigue Crack Propagation in Light Alloy Sheet Material and Structures. Rep. MP.195, Nationaal Luchtvaartlaboratorium (Amsterdam), Aug. 1960.

6. Hoag, J. G., Roach, D. B., and Hall, A. M.: Mechanical- and Physical-Property Data on Modified 12 Per Cent Chromium Martensitic Stainless Sheet Steels for Airframe Applications. DMIC Memo. 15, Battelle Memorial Inst., Apr. 18, 1959.

7. McEvily, Arthur J., Jr., Illg, Walter, and Hardrath, Herbert F.: Static Strength of Aluminum-Alloy Specimens Containing Fatigue Cracks. NACA TN 3816, 1956.

8. Irwin, G. R., Kies, J. A., and Smith, H. L.: Fracture Strengths Relative to Onset and Arrest of Crack Propagation. Proc. ASTM, vol. 58, 1958, pp. 640-657.

9. McEvily, Arthur J., Jr., and Illg, Walter: The Rate of Fatigue-Crack Propagation in Two Aluminum Alloys. NACA TN 4394, 1958.

TABLE I

NOMINAL COMPOSITION OF 12 MoV STAINLESS STEEL IN PERCENT WEIGHT

Carbon, C	0.25
Manganese, Mn	0.50
Silicon, Si	0.50
Chromium, Cr	12.0
Nickel, Ni	0.5
Molybdenum, Mo	1.0
Vanadium, V	0.3

TABLE II

HEAT TREATMENT OF 12 MoV STAINLESS-STEEL SPECIMENS

Condition	Austenitize	Temper
Decarburized 0.025 inch thick	1,850° F for 15 minutes; air atmosphere; air cool	900° F for 4 hours; air cool
Normal 0.031 inch thick	1,850° F for 20 minutes; dry hydrogen atmosphere; air cool	900° F for 4 hours; air cool

0.031-inch-thick 12 MoV stainless steel; normal condition; transverse cross-section edge; Marble's etch; ×250.

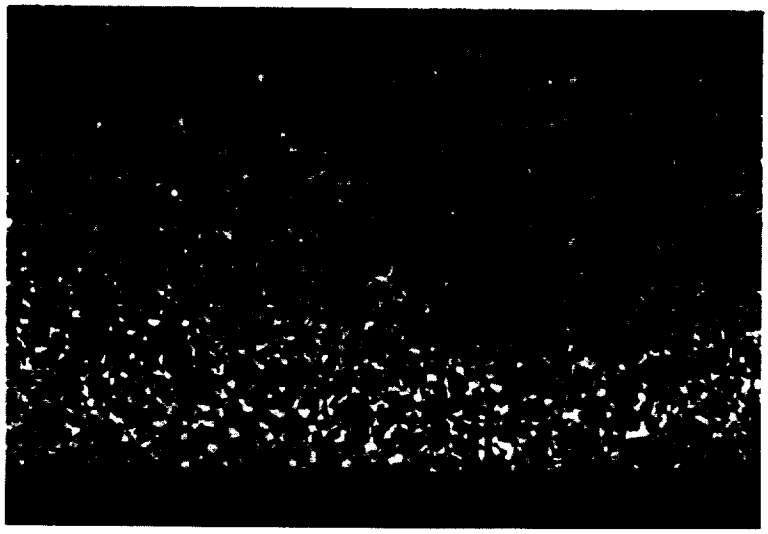

0.025-inch-thick 12 MoV stainless steel; decarburized condition; transverse cross-section edge; Marble's etch; ×250.

L-61-5065

Figure 1.- Microstructure of 12 MoV stainless-steel sheet in normal and decarburized conditions.

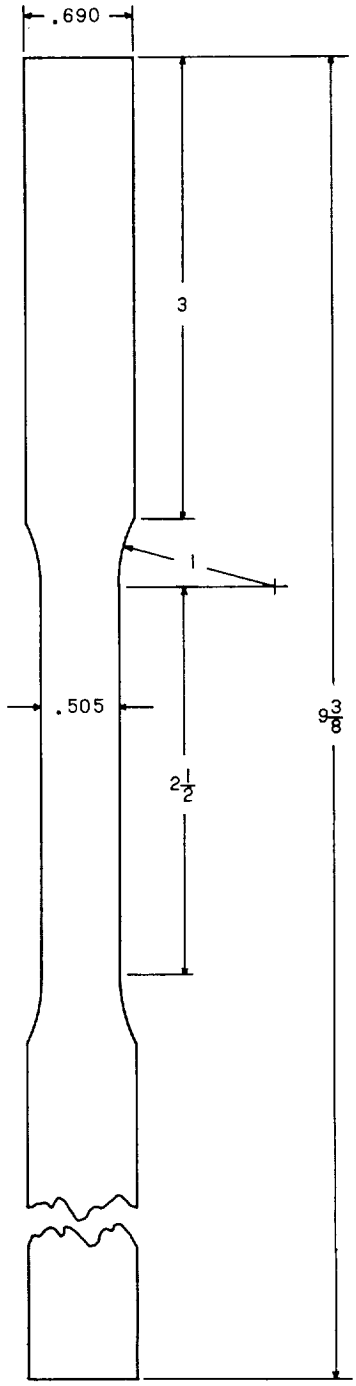

(a) Standard sheet tensile specimen.

Figure 2.- Configurations of specimens. All dimensions are in inches.

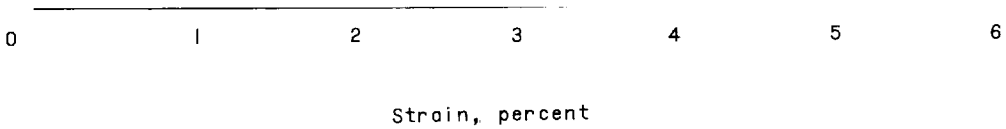

18

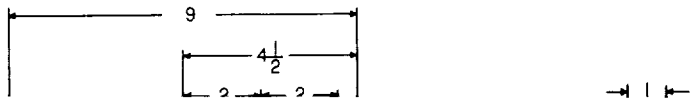

20

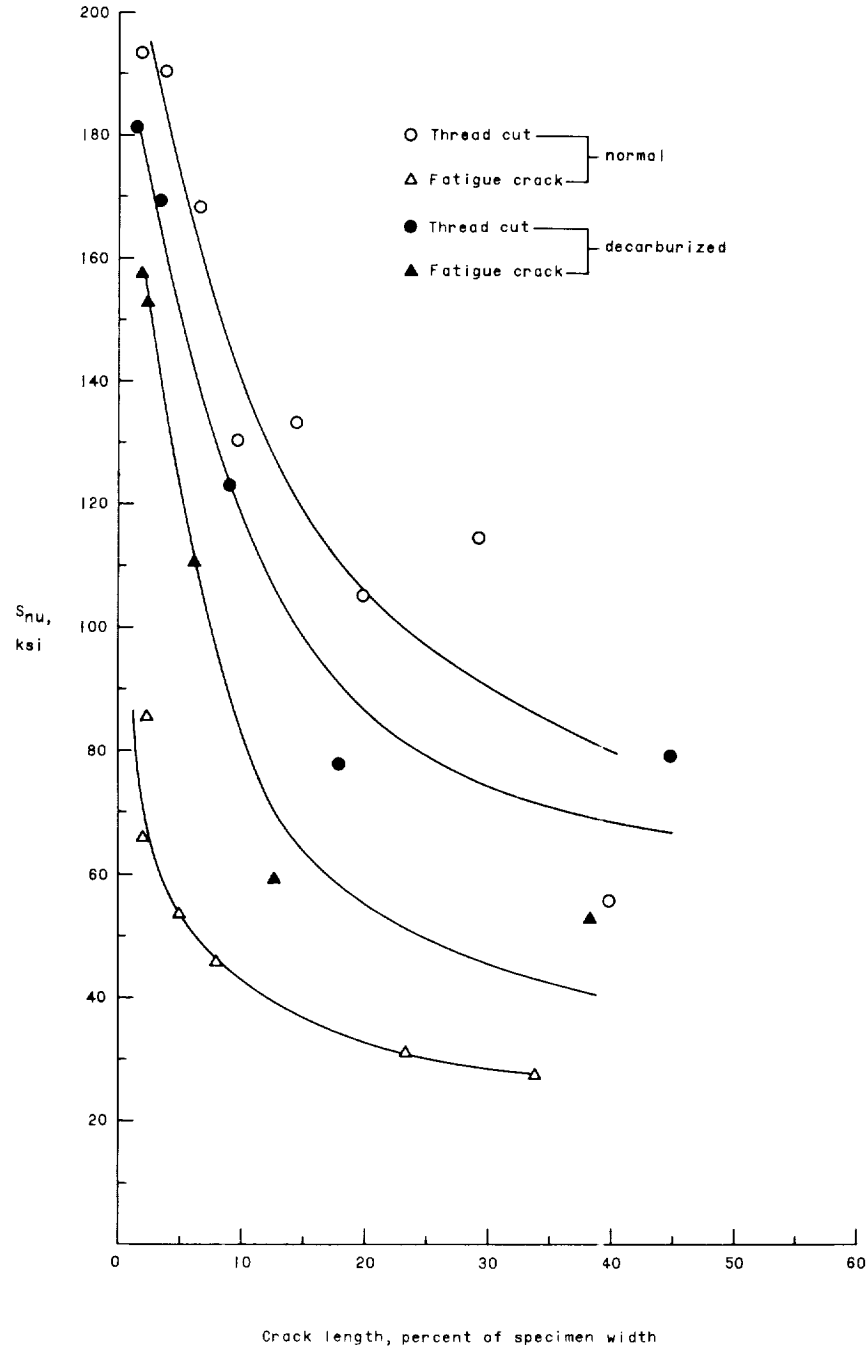

L-1354

Figure 4.- Effect of thread-cut notches and fatigue cracks on residual

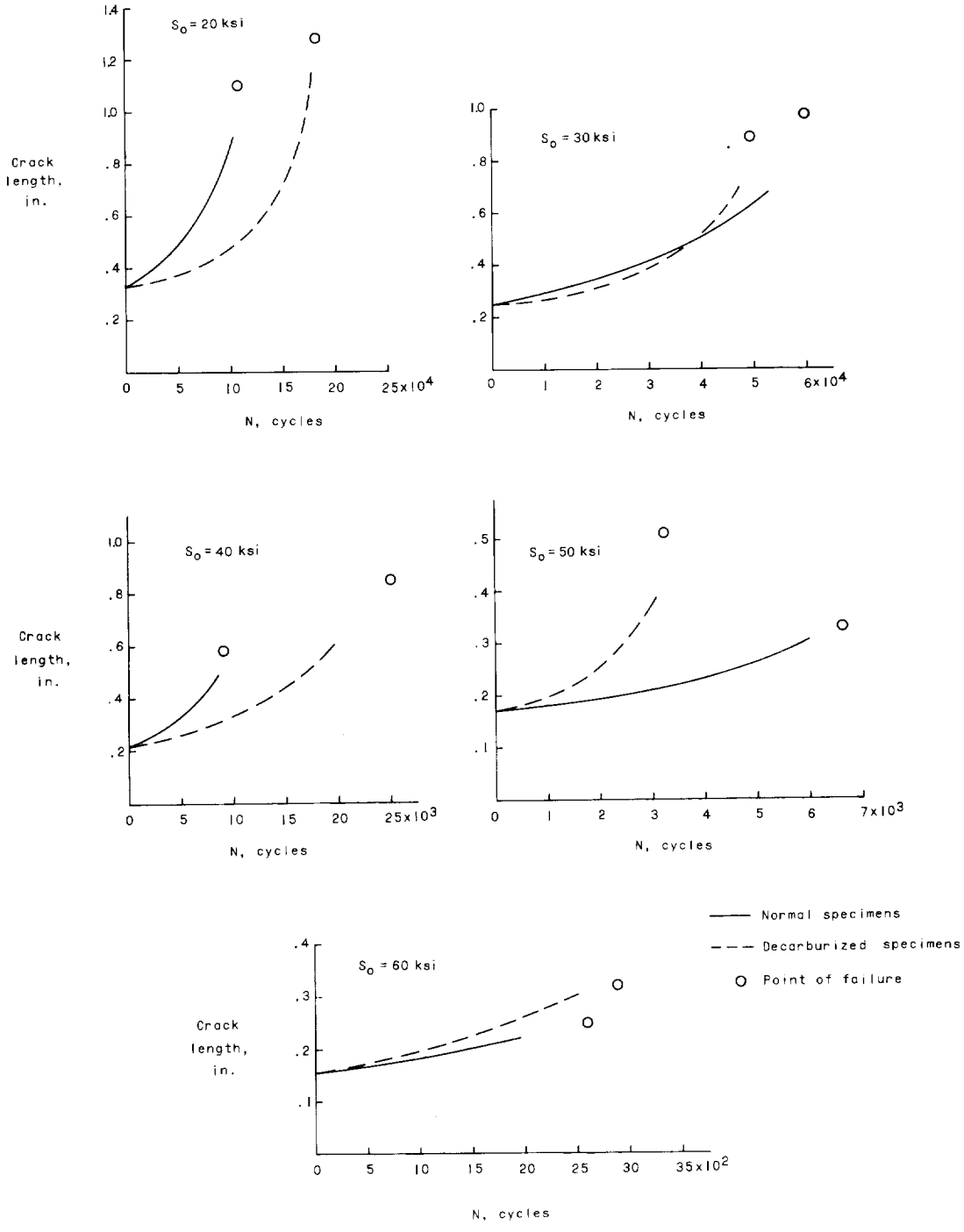

Figure 5.- Fatigue crack propagation curves for 12 MoV stainless-steel specimens, 2 inches wide.

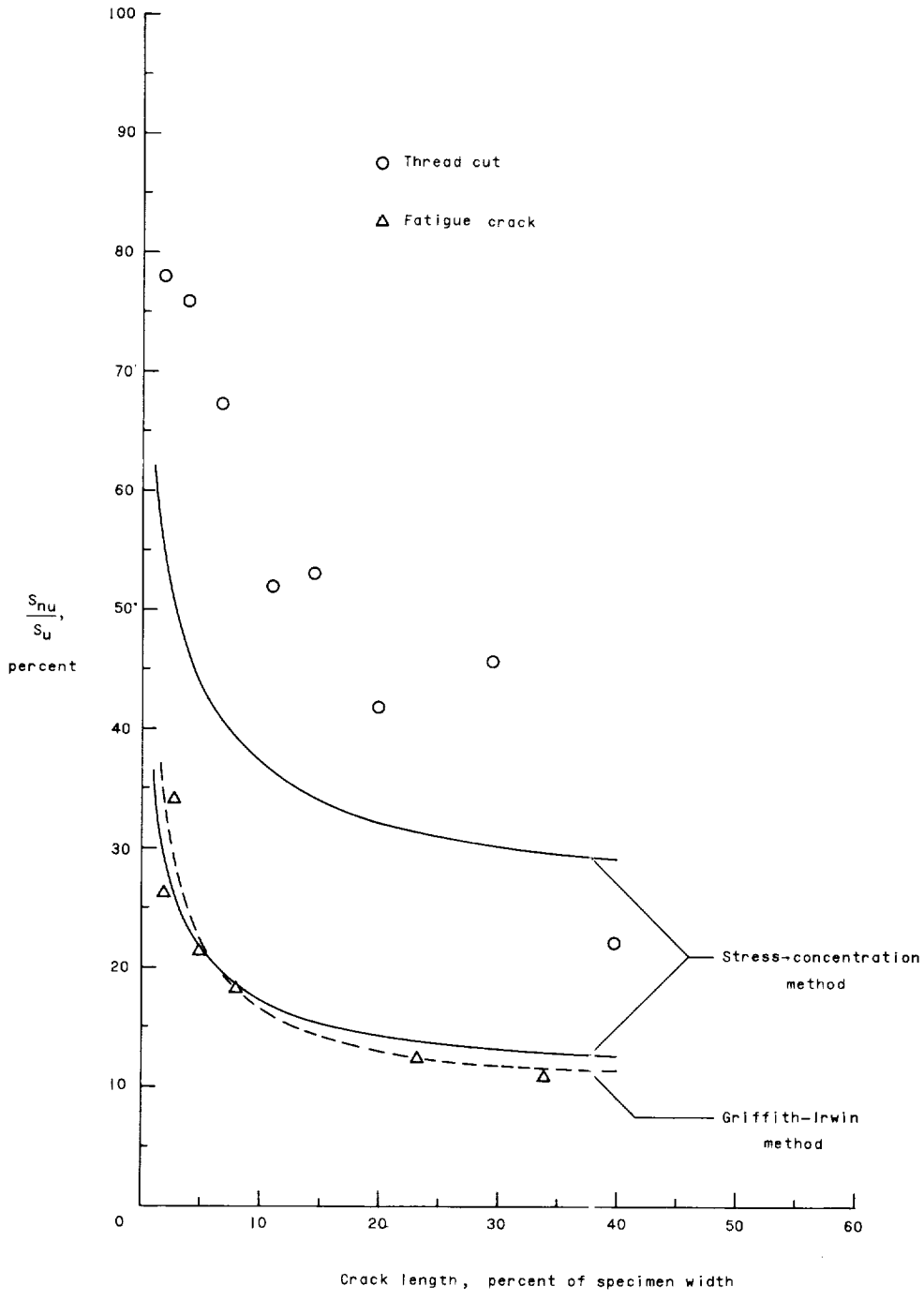

Figure 6.- Predicted and experimental results for residual static strength of normal 12 MoV stainless-steel specimens, 9 inches wide.

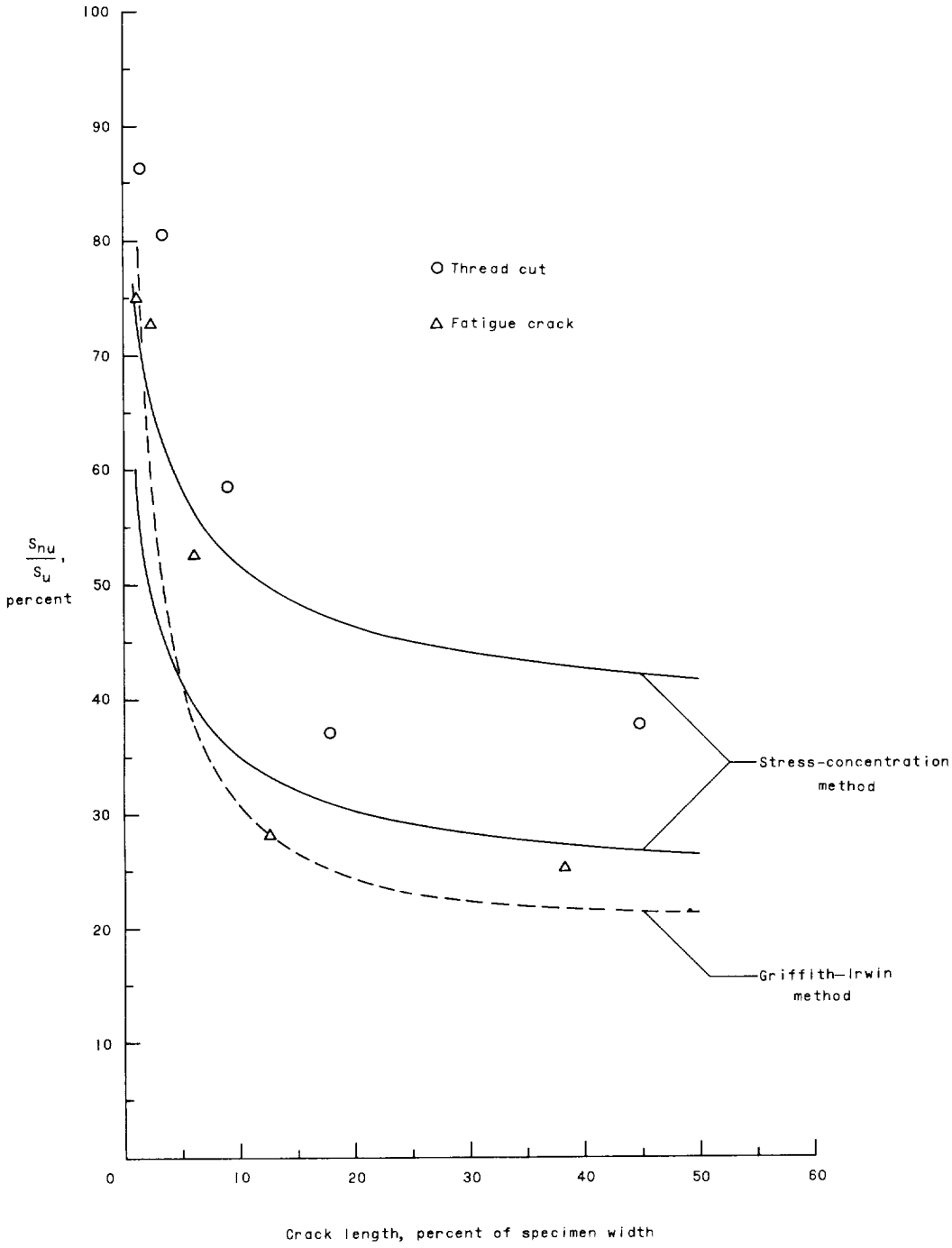

Figure 7.- Predicted and experimental results for residual static strength of decarburized 12 MoV stainless-steel specimens, 9 inches wide.

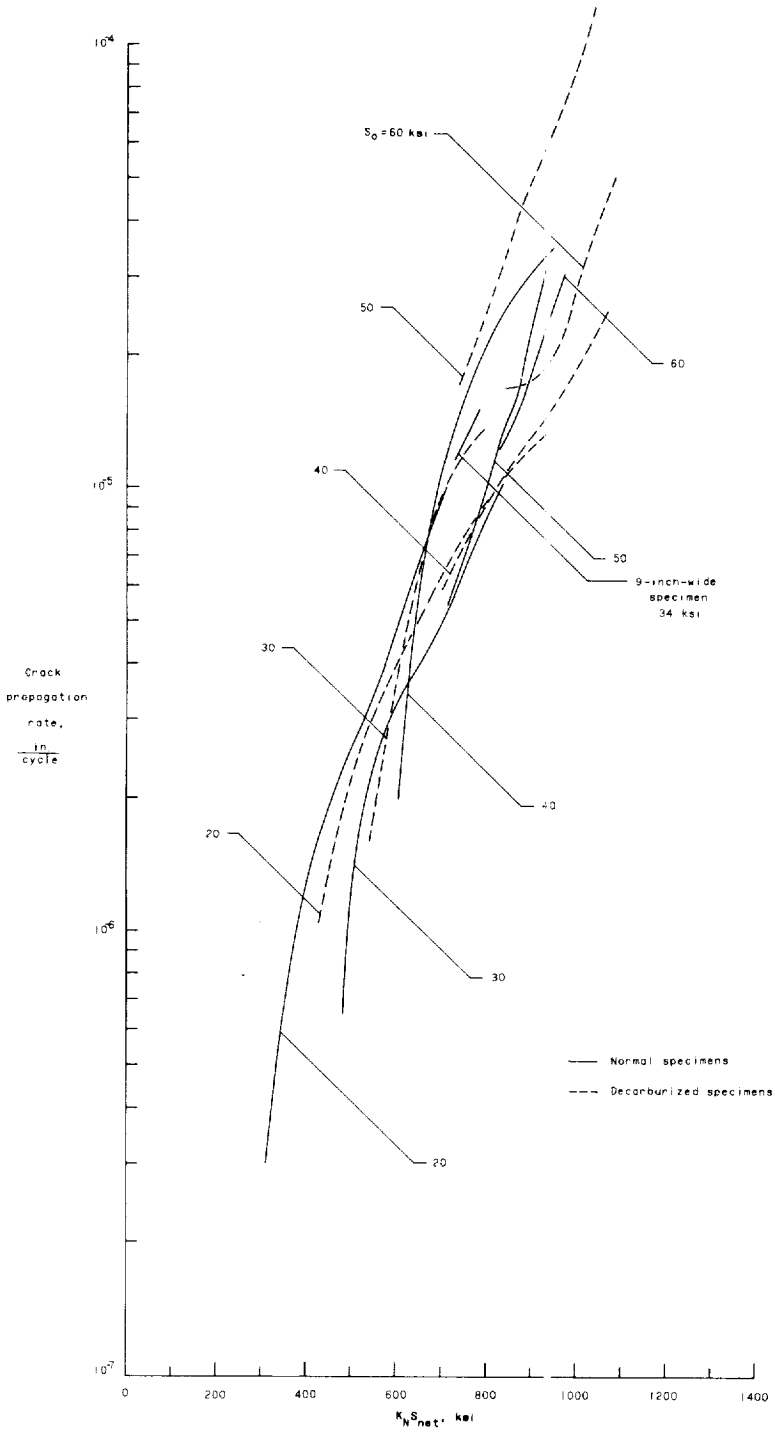

Figure 8.- Rates of fatigue crack propagation in 12 MoV stainless-steel specimens, 2 inches wide.

NASA-Langley, 1961 L-1354

L-1354